Eur. Phys. J. B **51**, 501–506 (2006)
DOI: 10.1140/epjb/e2006-00250-6

THE EUROPEAN PHYSICAL JOURNAL B

Fabrication and magnetic behaviour of 2D ordered Fe/SiO_2 nanodots array

W. Liu[1,2], W. Zhong[1,a], L.J. Qiu[1], L.Y. Lü[1], and Y.W. Du[1]

[1] National Laboratory of Solid State Microstructures, Jiangsu Provincial Laboratory for NanoTechnology, Nanjing University, Nanjing 210093, P.R. China
[2] College of Science, South China Agriculture University, Guangzhou 510642, P.R. China

Received 2 November 2005 / Received in final form 16 March 2006
Published online 22 June 2006 –

Abstract. We have demonstrated a simple and universal morphology-controlled growth of 2D ordered Fe/SiO_2 magnetic nanodots array, which was based on 2D colloidal monolayer template composed of polystyrene (PS) spheres and one-step sol-gel spin-coating technique. The Fe/SiO_2 nanodots have a well-ordered structure arranged in a hexagonal pattern. The dots have the shape of quasi-pyramidal tetrahedron, which reside in the interstitial region between three PS spheres and the substrate. Magnetic measurements reveal that the nanodots array exhibits the in-plane easy magnetization direction. Compared with the unpatterned Fe/SiO_2 thin film, the dots array has lower saturated field, higher remanence and coercivity. The present method is applicable to 2D ordered nanodots array of other magnetic materials.

PACS. 75.50.Bb Fe and its alloys – 75.75.+a Magnetic properties of nanostructures – 81.07.-b Nanoscale materials and structures: fabrication and characterization

1 Introduction

In recent years, the research on the magnetic dot arrays has drawn a great deal of interest from the viewpoint of fundamental micromagnetism as well as possible applications in magnetic storage media and magnetoelectronic devices [1,2]. These ordered nanostructures often manifest magnetic properties absent in bulk magnets or continuous thin films. Several groups have fabricated magnetic nanodots arrays and investigated their magnetic properties [3–6]. Many methods have been adopted to fabricate nanodots arrays, such as ion or electron lithography. However, the nanolithography is an expensive and painstaking step-by-step process. Recently, much attention has been directed towards self-assembly method, which is a much simpler and economic alternative [7,8]. Thereinto, methods based on templates formed by the self-assembly of colloidal particles have demonstrated promise for a number of new functional materials such as photonic materials, microchip reactors and biosensors [9–12]. Self-assembled nanofabrication processes with colloidal particles have advantages in that they are inexpensive, inherently parallel, and high-throughput processes [13,14]. Two-dimensional (2D) colloid crystals, especially colloidal monolayers, have been widely explored as sacrificial templates in creating regular arrays of nanopatterns [15,16].

Most of the current works on magnetic dots arrays are based on magnetic metals or alloys [17–21], such as metal Co, CoCrPt alloy and Co/Pt multilayer. However, only few were devoted to the research based on metal Fe. Metal Fe is good soft magnetic material with high saturation magnetization. Due to its intrinsic property of the finely divided metal, it could be oxidized in air very easily even at room temperature, which limits its applications. To solve the problem, we have successfully covered the metallic nanoparticles by silica or alumina shell to create the core-shell nanocomposite structures in our previous works [22,23].

In this paper, the aim of this work is to obtain a regular array of Fe/SiO_2 nanostructures with a narrow size distribution via a self-organized growth process. In our process monodisperse polystyrene (PS) nanospheres were used as templates. The interstices between the close-packed PS spheres assembly formed an array with hexagonal shape in a single layer. The interstices were used for infiltration of the metal by sol-gel method. After heat treated, the dots array was formed.

There have been some works to fabricate magnetic nanostructures prepared by sol-gel or electrochemical deposition through colloidal templates. But most of them are "networks" structures, other than periodical dots arrays. As far as we know there are no other reports to form the dots array by our strategy. It is of practical significance in magnetic devices since the magnetic properties of metal

[a] e-mail: wzhong@nju.edu.cn

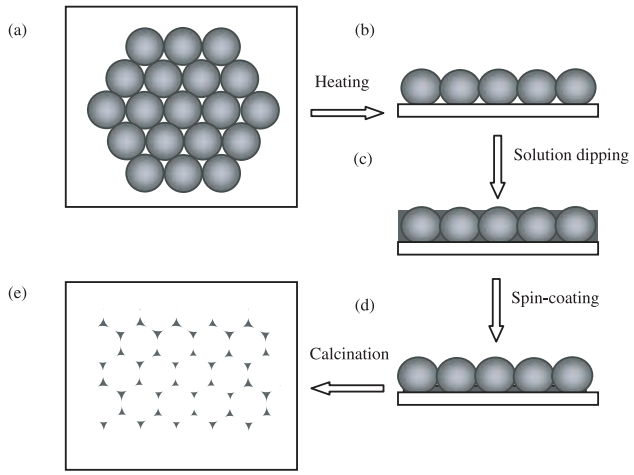

Fig. 1. Schematic illustrations of the fabricating process for nanodots array: (a) a monolayer of polystyrene spheres were spread onto the substrate; (b) the substrate with the monolayer were heated in an oven at 100 °C to bond the monolayer to the substrate; (c) the precursor solution was dropped onto the polystyrene template; (d) the precursor solution penetrated the voids of the colloidal crystals by spin-coating method; (e) after calcination the nanodots array with "quasi-pyramidal tetrahedron-shaped" structures arranged in a honeycomb pattern were formed and the polystyrene spheres were decomposed.

dots are sensitive to the morphology of the nanostructures. The key of our strategy is the treating condition, which was controlled accurately to avoid the pattern loss. The components, microstructure, and magnetic properties of the dots array were investigated. The formation mechanism of the ordered array structure was also discussed.

2 Experimental

Figure 1 schematically illustrates how Fe/SiO_2 nanodots array can be prepared by a template-assisted method. First, a colloidal monolayer array composed of polystyrene spheres was prepared on a quartz plate from an aqueous suspension of polystyrene spheres (Alfa Aesar Corporation) by spin-coating method (Fig. 1a). The diameter of the spheres was 1 μm, and the concentration of the suspension was 2.5 wt%. Then, the substrate with the monolayer was heated in an oven at 100 °C for some minutes to bond the monolayer to the substrate. Doing this, a monolayer of hexagonally arranged PS spheres was produced.

The key consideration in the synthesis of the Fe/SiO_2 nanoparticles was to make a precursor solution that easily infiltrated the interstitial voids in the PSs colloid of the template and that adhered strongly to the template via a condensation reaction. Moreover, in order to prevent oxidation of the iron, tetraethyl orthosilicate (TEOS) was used as the raw material to form a protected SiO_2 shell on the surface of the as-prepared Fe nanoparticles [22]. We employed a sol-gel method in our synthetic process to achieve filling of the template. After the precursor solution

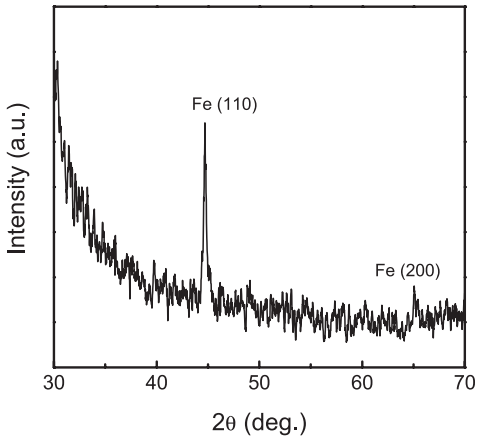

Fig. 2. X-ray diffraction pattern of Fe/SiO_2 nanodots array film.

was prepared [22], the precursor solution was then gently dropped into the polystyrene template and penetrated the voids of the colloidal crystal by spin-coating at 3500 rpm and for 60 s. After dried in an oven at 90 °C for 1 h, the filled template was slowly heated to 450 °C (heating rate: 2 °C/min) and sintered at this temperature for 2 h in the air, then reduced in flowing H_2 gas at 800 °C for 4 h.

For the purpose of comparison, Fe/SiO_2 thin film was prepared direct on the quartz substrate without PSs colloidal template from the same precursor solution under identical conditions.

The phase identification and structure analysis of the films were examined by X-ray powder diffraction (XRD) with Cu-Kα radiation (Model D/Max-RA, Rigaku, Japan). Surface morphology was carefully examined via a scanning electron microscope (SEM JSM-5610LV), and atomic force microscope (AFM Nanoscope IIIa). Magnetic measurements were performed at room temperature using a superconducting quantum interference device (SQUID, Quantum Design).

3 Results and discussion

The phase purity of the Fe/SiO_2 nanodots array was checked by the X-ray powder diffraction, which is given in Figure 2. The Fe (110) and (200) peak in the curve indicates that pure Fe with cubic-phase structure exists in the structure of the dots array film. No peak of crystalline SiO_2 is found in the sample.

Figure 3 presents typical SEM and AFM images of the microstructured Fe/SiO_2 nanodots array which was successfully prepared over areas of 5 mm $\times$ 5 mm by our method. The SEM and three-dimensional AFM image (Figs. 3a, 3b) demonstrates that the Fe/SiO_2 nanodots have a well-ordered structure arranged in a honeycomb pattern. From the more highly magnified AFM top-view image (Fig. 3c), it is clearly seen that Fe/SiO_2 particles appear quasi-pyramidal tetrahedron-shaped structures with average diameters (at the bottom) of approximately 350 nm, which reside in the interstitial region between

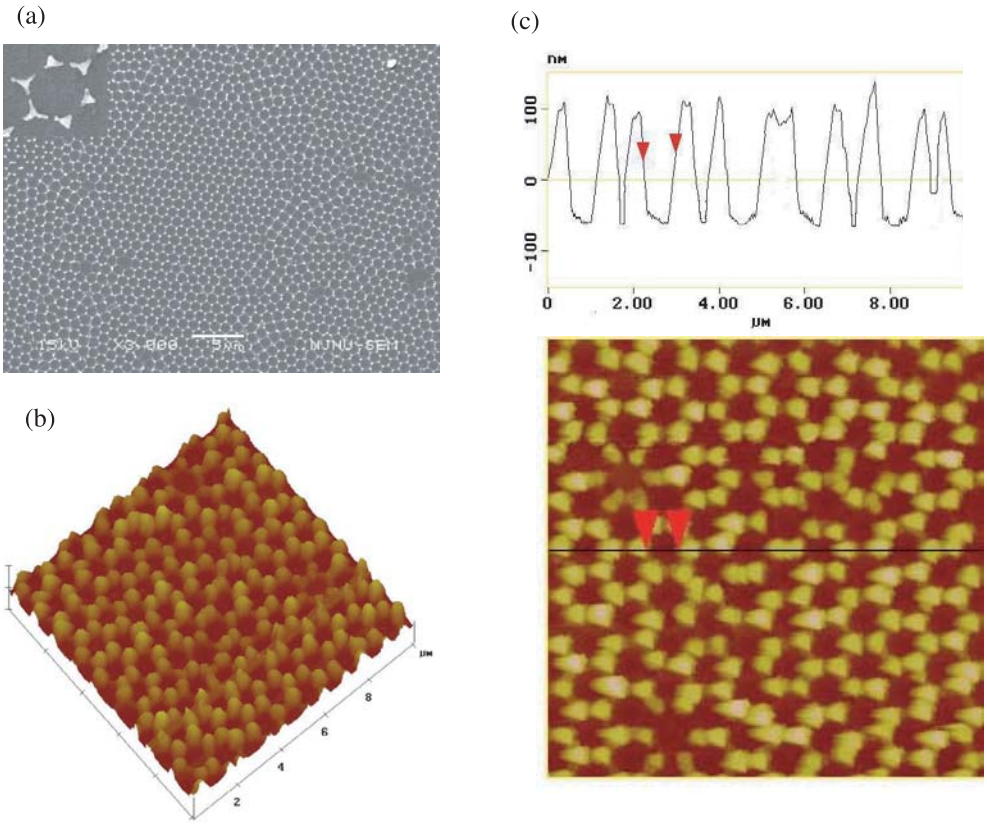

Fig. 3. (a) SEM images, and (b, c) tapping mode AFM images of Fe/SiO_2 dots array: (b) three-dimensional image, and (c) top-view image and section analysis.

three spheres and the substrate. From the AFM surface contour of the array film, these quasi-pyramidal tetrahedron-shaped dots are not touching each other and exhibit center-to-center distance around 600 nm. The average height of the dots (the peak-to-valley distance) was about 150 nm.

These nanodots arranged periodically. Every six of the quasi-pyramidal tetrahedron-shaped nanodots surround the position where the latex sphere was originally located on the substrate and hence they are also arranged in hexagon. From the AFM section analysis, the diameter of the voids was about 900 nm at the top and 400 nm at the bottom. The distance between adjacent pores (center-to-center) is always closer to the diameter of the PSs (1000 nm). The periodicity of arranged Fe/SiO_2 dots array was in agreement with the interstices pattern between the ordered PS spheres.

The final structure and morphology of the ordered dots array depend on several factors. Changes in the shape of the PSs during heating are essential to the morphologies. The sticking behavior of the precursor solution and spin-coating speed and time are also crucial.

The substrate coated with the colloidal monolayer was preheated in an oven to 100 °C, which is higher than the glass transition temperature of polystyrene [24]. Such heating induces an area contact, instead of a point contact, between the PSs. And this enlarged area contact increases the binding force between the PSs and the substrate, which is important for the subsequent treatment since the ordered monolayer would not be destroyed by spin-coated process. When the precursor solution is dropped onto the colloidal monolayer template, the interstitial spaces of the closely packed PSs are then filled with the solution due to capillary action, as illustrated schematically in Figure 1. After spin-coated, by control of the spin-coating speed and time, the precursor solution will mainly reside in the wedge-shaped region between the PSs and the substrate. When drying at 90 °C for 1 h and calcinating by slow temperature-rising speed, the PSs was deformed further, with greatly increased contact between neighboring spheres. Meanwhile, with the solvent evaporating, the gel precipitated and shrank. Finally, nearly triangular disconnected sediments are left between three adjacent deformed spheres and the substrate due to lack of sufficient solution compensation. Then all organics decomposed below 450 °C in air.

There are still some defects in the dots array, which are mainly due to the inherent polydispersity of the PSs. If the adjacent PS colloids are not in contact closely in the original templates, the deposited material filled interstitials to form connected dots rather than distinct ones. The assembly of the colloidal crystals is usually the (111) arrangement. Occasionally, other orientations, such as (100), are also seen. Then four nodes every group, instead of six, appeared periodically at the interstitial positions of the adjacent two PS spheres (Fig. 3a).

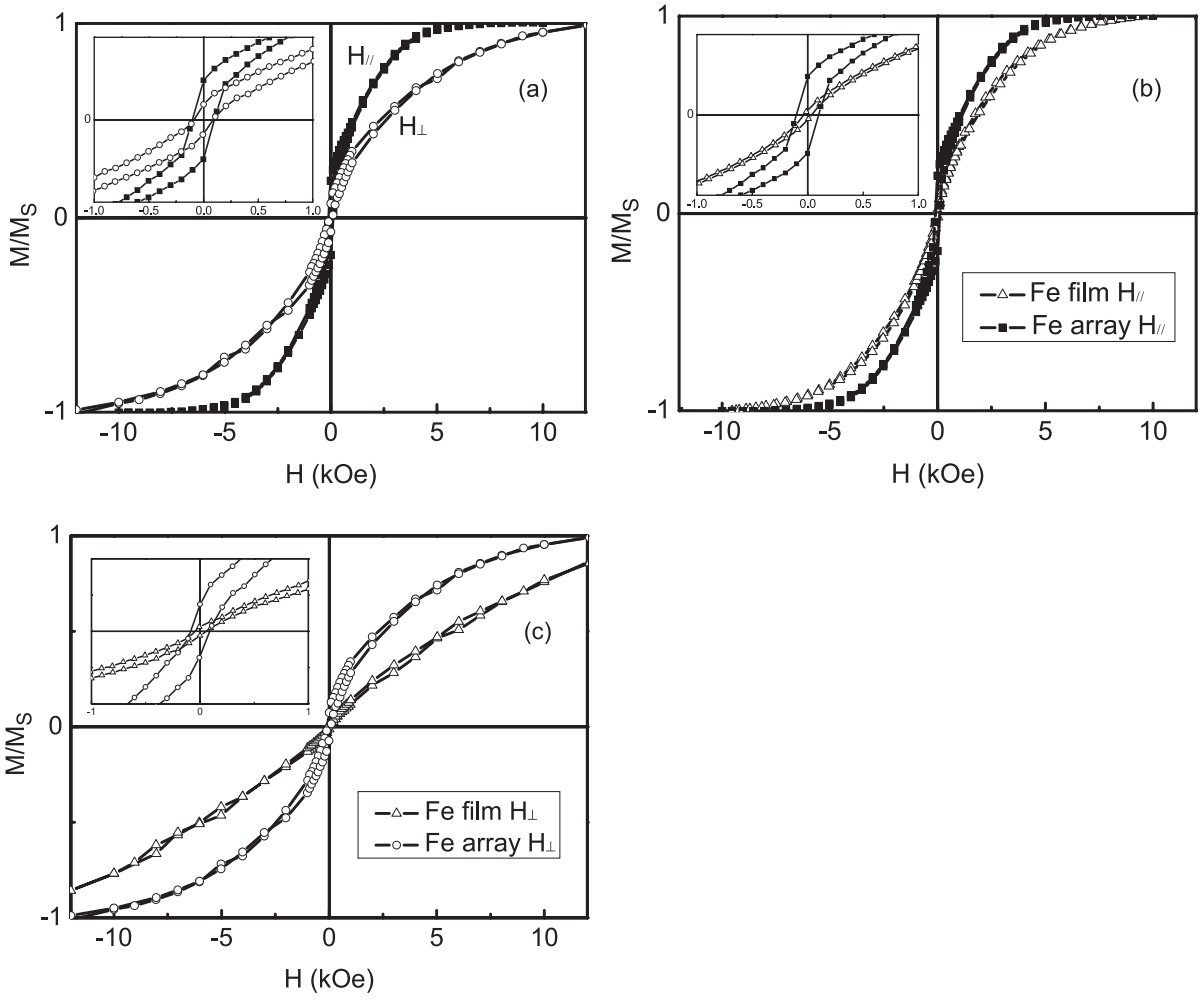

Fig. 4. Hysteresis loops at room temperature for (a) 2D ordered Fe/SiO_2 dots array with the applied field parallel and perpendicular to the plane; (b) the Fe/SiO_2 thin film and the Fe/SiO_2 dots array with the applied field parallel to the plane; (c) the Fe/SiO_2 thin film and the Fe/SiO_2 dots array with the applied field perpendicular to the plane. Inset shown are around origin. The moment is normalized to the saturation magnetization of each sample.

Figure 4a shows the $M-H$ hysteresis loops of the nanodots array measured at room temperature, after subtracting the linear diamagnetic background due to silica. The external magnetic field was applied parallel (in-plane) and perpendicular (out-of-plane) to the plate plane. The ferromagnetic property of the nanodots array is observed from the hysteresis loop. It also can be found that when the applied field is parallel to the plane, the nanodots array can be saturated at a lower field of about 6 kOe. Meanwhile, the value of the magnetic remanence (Mr/Ms) for in-plane magnetization is 0.19, higher than that of out-of-plane. These facts indicate that the easy magnetization direction of the dots array is in-plane.

For comparison, Fe/SiO_2 thin film was prepared direct on the quartz substrate without PSs template under the same reaction conditions. The film thickness is about 130 nm. Here, both the Fe/SiO_2 thin film and dots array are made up of the Fe/SiO_2 nanoparticles (∼45 nm) with core-shell structures, in which each one of the Fe nanoparticles is surrounded by SiO_2 as separating shell. In order to understand the difference of magnetic properties between the thin film and the dots array, we present in Figures 4b and 4c their hysteresis loops with the applied field parallel and perpendicular to the plane. It could be observed that the dots array has lower saturation field, higher remanence and coercivity compared with the Fe/SiO_2 thin film (see Tab. 1).

Table 1. The magnetic properties of the dots array and the film for in-plane and out-of-plane.

	In-plane		Out-of-plane	
	Array	Film	Array	Film
H_S (kOe)[a]	6	10	12	>12
H_C (kOe)	110	45	73	23
Mr/Ms	0.19	0.02	0.08	0.008

[a] Saturation field.

It is generally recognized that the magnetization reversal process in a real ferromagnet is dominated by the energy terms, which are composed of exchange, magnetocrystalline anisotropy, and magnetostatic contributions [25]. In both the nanodots array and thin film, the magnetocrystalline anisotropy of polycrystalline Fe nanoparticles is low and could be neglected. In addition, between the Fe nanoparticles, exchange coupling interaction is not considered since magnetic core Fe is separated by silica shell with 3–5 nm thickness. Therefore, the magnetostatic coupling interaction (i.e. the magnetic dipolar interaction) plays a major role in determining the magnetic behavior of the nanoparticles. It was found in recent articles that magnetostatic interaction between soft magnetic elements becomes important when the particles are dense and particle separations are less than the lateral particle sizes [5,26]. For the same materials, magnetostatic interactions are relative to the size, shape, amount, and distance of the particles. In the dots array, there are many vacancies among the dots since the special structural arrangement of the Fe/SiO_2 nanoparticles. The amount of the magnetic nanoparticles in a unit area of the array sample is much less than that in the film. So, the average magnetostatic interaction in the array is lower than that in the film. Generally speaking, during magnetization process magnetostatic interaction tends to hamper the magnetic dipolars to align parallel but favor them to rotate back in the magnetization reversal process. The stronger the magnetostatic interaction is, the more evident the shearing effect of the magnetic loop becomes. Accordingly, the saturation field of the thin film is higher, but the remanence and coercivity are lower.

The collective magnetic behaviour of the Fe/SiO_2 nanodots array is determined both by the magnetic properties of the individual particles and by their arrangement in three dimensions. There are many factors should be considered, such as the shape anisotropy, which may play an important role in determining the magnetic state of the nanostructures, especially for polycrystalline systems. Additionally, surface anisotropy (due to the change in coordination number of the surface atoms) may also affect the magnetic properties. The surface-to-volume ratio is high in dots. The reduction in coordination numbers of the surface atoms can introduce frustration and spin disorder [27], therefore, strongly modify the magnetic anisotropy relative to the bulk and film material. Although nominally identical, the dots may still have small differences, either due to the preparing process or different grain structures, resulting in different edge roughness or other kinds of random defects. The imperfection or defect in the structure and their boundaries can act as magnetic impurities, and edge roughness can also pin the magnetization, which could affect the magnetization reversal.

Metal Fe nanoparticles could be oxidized in air very easily even at room temperature. The silica shell on the surface could protect Fe core from oxidization. Figure 5 shows the weight change of the Fe/SiO_2 nanodots array when it was heated in air. It indicates that its weight almost kept unchanged below 200 °C. Due to the protection of the silica shell, the iron nanodots array kept very stable in air.

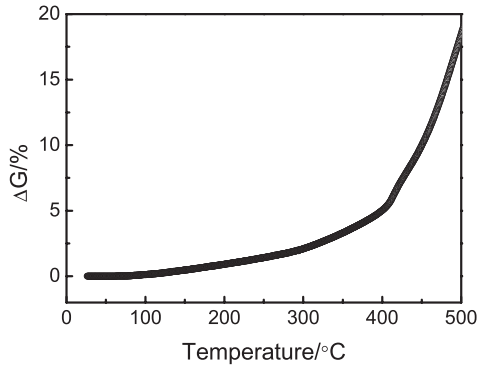

Fig. 5. Thermal gravity curve of the Fe/SiO_2 nanodots array.

4 Conclusions

In summary, we have successfully fabricated highly-ordered Fe/SiO_2 nanodots array via sol-gel method by the self-assembled PSs colloidal template. The morphology of the 2D nanostructures was controlled by adjusting treatment conditions, including the concentration of the precursor solution, heating treatment and spin-coating speed and time. In the magnetic measurements, the nanodots array exhibits the easy magnetization direction parallel to the plate plane. Especially, the Fe/SiO_2 dots array had lower saturation field, higher coercivity and remanent magnetization than the Fe/SiO_2 thin film. It shows that the magnetic behavior of nanostructure arrays can be understood by considering the collective properties of the nanoparticles. A full understanding of the magnetic behavior of the dots array will require deep studies of the effect of size, shape, and microstructure of the dots, and the geometry of the array which governs magnetostatic interactions between the dots. This fabrication method is very simple and easy-controlled and can be extended to the preparation of other functional materials with the same configuration.

This work was supported by the National Natural Science Foundation of China under Grant No. 50471049, and the National Key Project for Basic Research (No. 2005CB623605), People's Republic of China.

References

1. Y.S. Chou, Proc. IEEE **85**, 652 (1997)
2. J.Y. Cheng, W. Jung, C.A. Ross, Phys. Rev. B **70**, 064417 (2004)
3. C.A. Ross, H.I. Smith, T. Savas et al., J. Vac. Sci. Technol. B **17**, 3168 (1999)
4. A. Fernandez, P.J. Bedrossian, S.L. Baker, S.P. Vernon, D.R. Kania, IEEE Trans. Magn. **32**, 4472 (1996)

5. V. Novosad, K.Y. Guslienko, H. Shima et al., Phys. Rev. B **65**, 060402 (2002)
6. R. Zhu, Y.T. Pang, Y.S. Feng, G.H. Fu, Y. Li, L.D. Zhang, Chem. Phys. Lett. **368**, 696 (2003)
7. Mikrajuddin, F. Iskandar, K. Okuyama, Adv. Mat. **14**, 930 (2002)
8. M.S. Sander, L.S. Tan, Adv. Func. Mat. **13**, 393 (2003)
9. Y.A. Vlasov, X.Z. Bo, J.C. Sturm, D.J. Norris, Nature **414**, 289 (2001)
10. H. Gau, S. Herminghaus, P. Lenz, R. Lipowsky, Science **283**, 46 (1999)
11. Z.P. Huang, D.L. Carnahan, J. Rybcynski, M. Giersig, M. Sennett, D.Z. Wang, J.G. Wen, K. Kempa, Z.F. Ren, Appl. Phys. Lett. **82**, 460 (2003)
12. P. Jiang, J.F. Bertone, V.L. Colvin, Science **291**, 453 (2001)
13. A. Kosiorek, W. Kandulski, P. Chudzinski, K. Kempa, M. Giersig, Nano Lett. **4**, 1359 (2004)
14. C.L. Haynes, R.P. Van Duyne, J. Phys. Chem. B **105**, 5599 (2001)
15. J.E. Barton, T.W. Odom, Nano Lett. **4**, 1525 (2004)
16. J.M. McLellan, M. Geissler, Y.N. Xia, J. Am. Chem. Soc. **126**, 10830 (2004)
17. D.G. Choi, J.R. Jeong, K.Y. Kwon, H.T. Jung, S.C. Shin, S.M. Yang, Nanotechnology **15**, 970 (2004)
18. A. Goncharova, A.A. Zhukova, P.N. Bartlettb, M.A. Ghanemb, R. Boardmanc et al., J. Magn. Magn. Mater. **286**, 1 (2005)
19. D.G. Choi, S. Kim, S.G. Jang, S.M. Yang, J.R. Jeong, S.C. Shin, Chem. Mater. **16**, 4208 (2004)
20. W. Kipferl, M. Dumm, M. Rahm, G. Bayreuther, J. Appl. Phys. **93**, 7601 (2003)
21. Y. Sasaki, M. Mizuno, A.C.C. Yu et al., IEEE Trans. Magn. **41**, 660 (2005)
22. N.J. Tang, W. Zhong, W. Liu, H.Y. Jiang, X.L. Wu, Y.W. Du, Nanotechnology **15**, 1756 (2004)
23. W. Liu, W. Zhong, H.Y. Jiang, N.J. Tang, X.L. Wu, Y.W. Du, Eur. Phys. J. B **46**, 471 (2005)
24. Y. Yin, Y. Lu, Y. Xia, J. Am. Chem. Soc. **123**, 771 (2001)
25. A. Aharoni, *Introduction to the Theory of Ferromagnetism* (Oxford University Press, New York, 2001)
26. M. Natali, I.L. Prejbeanu, A. Lebib, L.D. Buda, K. Ounadjela, Y. Chen, Phys. Rev. Lett. **88**, 157203 (2002)
27. R.H. Kodama, S.A. Makhlouf, A.E. Berkowitz, Phys. Rev. Lett. **79**, 1393 (1997)